A particle-filter information potential method for tracking and monitoring maneuvering targets using a mobile sensor agent

W. Lu, G. Zhang, S. Ferrari, M. Anderson and R. Fierro

The Journal of Defense Modeling and Simulation: Applications, Methodology, Technology published online 1 June 2012
DOI: 10.1177/1548512912445406

Original Article

JDMS

Journal of Defense Modeling and Simulation: Applications, Methodology, Technology
1–12

DOI: 10.1177/1548512912445406
dms.sagepub.com
SAGE

A particle-filter information potential method for tracking and monitoring maneuvering targets using a mobile sensor agent

W Lu[1], G Zhang[1], S Ferrari[1], M Anderson[2] and R Fierro[2]

Abstract

The problem of tracking and monitoring moving targets using mobile sensor agents (MSAs) is relevant to a variety of applications, including monitoring of endangered species, civilian security, and military surveillance. This paper presents a new information potential field approach for computing the motion plans and control inputs of a MSA, based on the feedback obtained from a modified particle filter used for tracking multiple moving targets in a region of interest. A modified particle filter is presented that implements a new sampling method based on supporting intervals of normal probability density functions. The method accounts for the latest sensor measurements by adapting a mixture representation of the target probability density functions (PDFs). The target motion is modeled as a semi-Markov jump process, such that the target PDFs, or the PDFs of the Markov parameters, can be updated based on real-time sensor measurements by a centralized processing unit or MSAs supervisor. A new information potential method is presented that computes an artificial potential function based on the output of the modified particle filter. Using this artificial potential, the sensors compute feedback control inputs that allow them to track and monitor a maneuvering target over time, using a bounded field of view (FOV).

Keywords

target tracking, monitoring, surveillance, mobile sensor networks, multi-agent systems, information value, potential field, particle filtering

1. Introduction

The problem of tracking and monitoring maneuvering targets using one or more mobile sensor agents is relevant to a variety of applications, including monitoring of urban environments,[1] tracking anomalies in manufacturing plants,[2] and tracking of endangered species.[3] A *mobile sensor agent* (MSA) is defined as an autonomous vehicle equipped with embedded wireless sensors and communication devices. Many modern surveillance systems deploy MSAs to detect and track moving targets based on limited information that only becomes available when the target enters the sensor's field of view (FOV) or visibility region. The sensor's FOV is defined as a compact subset of the region of interest (ROI), in which the sensor can obtain measurements from the targets. Similarly to traditional robot path planning methods which consider the geometries of the robots and obstacles to avoid collisions, in

[1] Laboratory for Intelligent Systems and Control (LISC), Department of Mechanical Engineering and Materials Science, Duke University, Durham, NC, USA
[2] Multi-Agent, Robotics, Hybrid, and Embedded Systems (Marhes), Laboratory Department of Electrical and Computer Engineering, University of New Mexico, Albuquerque, NM, USA

Corresponding author:
W Lu, Laboratory for Intelligent Systems and Control (LISC), Department of Mechanical Engineering and Materials Science, Duke University, Durham, NC, 27708, USA.
Email: wenjie.lu@duke.edu

sensor path planning it is possible to consider the geometries of the FOV and the targets to compute paths that enable sensor measurements.[4–7] In this paper, the MSA path plan and controls are computed such that the tracking performance of the sensor is optimized and such that, once a track is estimated, the MSA can maintain the moving target within its FOV for monitoring purposes.

Recently, cell decomposition[8] and probabilistic roadmap methods[6] have been developed for solving sensor path planning problems for stationary targets. A computational geometry approach has also been developed to maximize the probability of detection for moving targets in a pre-defined ROI.[9] Visibility-based methods have been proposed to account for the sensor's dynamics and FOV geometry in robot landmark navigation.[10–13] A hybrid method based on line transversals and cell decomposition has been developed to track and pursuit maneuvering targets using MSAs, in order to capture the targets once their tracks are formed from multiple detections.[14] Existing methods, however, do not account for the uncertainty associated with tracking a moving target that may be maneuvering unexpectedly at any time in the ROI. In fact, in addition to the uncertainty associated with environmental conditions and noisy sensor measurements, if a target unexpectedly changes heading and velocity, it may escape the sensor's FOV and never be detected again.

The information potential method developed in this paper allows the MSA's path plan and control to take into consideration a probabilistic model of the target maneuvers that is constantly updated with real-time measurements. Based on this model, and on the geometry of the FOV, the MSA path is computed such that the sensor can monitor the target. In other words, the information potential method maintains a predefined distance between the MSA platform and the target, such that the target remains inside the sensor's FOV at all times. The stability of the resulting sensor control law is guaranteed using Lyapunov stability theory. One approach to modeling moving targets in target tracking is to use a linear dynamical system with random disturbance inputs.[15–19] Then, under proper assumptions that include additive random noise with a Gaussian distribution, the target state can be estimated from frequent observations of its measurable output, using a Kalman filter.[20] This approach is well suited to long-range high-accuracy sensors, such as radars, and to moving targets with a known dynamical model and initial conditions. However, most of these underlying assumptions are violated in modern applications of MSAs, because the targets' motion models are unknown, and, possible, random and nonlinear. Also, due to the use of low-cost passive sensors, measurement errors and noise may be non-additive and non-Gaussian.

An extended Kalman filter (EKF) can be used when the system dynamics are nonlinear, but can be linearized about nominal operating conditions.[21] An unscented Kalman filter (UKF) method, based on the unscented transformation (UT) method, can be applied to compute the mean and covariance of a function up to the second order of the Taylor expansion.[22,23] However, the efficiency of these filters decreases significantly when the system dynamics are highly nonlinear, and when the random effects are non-Gaussian. Recently, a non-parametric method based on condensation and Monte Carlo simulation, known as a particle filter, has been proposed for tracking multiple targets exhibiting nonlinear dynamics and non-Gaussian random effects.[24] Particle filters are well suited to modern surveillance systems because they can be applied to Bayesian models in which the hidden variables are connected by a Markov chain in discrete time, but the target state is continuous, as in Markov motion models.

In the classical particle filter method, a weighted set of particles or point masses are used to represent the probability density function (PDF) of the target state by means of a superposition of weighted Dirac delta functions.[25] At each iteration of the particle filter, particles representing possible target state values are sampled from an importance density function.[26] The weight associated with each particle is then obtained from the target-state likelihood function, and from the prior estimation of the target state PDF. When the effective particle size is smaller than a predefined threshold, a re-sampling technique can be implemented.[27] One disadvantage of classical particle-filtering techniques is that the target-state transition function is used as the importance density function to sample particles, without taking new observations into account.[28] As a result, when the target state transition function is much broader than the likelihood function, few sampled particles have proper locations and weights. An improved particle filter, the unscented particle filter (UPF), has been proposed[28] to overcome this difficulty, by combining UKF and the particle-filtering technique. The UKF generates a proposed distribution in which the current measurements are considered, and then the distribution is used as the importance density to sample particles. Another disadvantage of existing particle filters is that the point-mass representation provides limited information about the estimated PDF of the target state, and does not account for the targets' dynamic equations.

This paper presents a new sampling method and a new representation for the approximation of the target state PDF that also accounts for the target dynamics. In the proposed method, the target dynamics are modeled by a semi-Markov jump process, and the particles are sampled based on the supporting intervals of the target-state likelihood function and the prior estimation function of the target state. In this case, the supporting interval of a distribution is defined as the 90% confidence interval.[29] The weight for each particle is obtained by considering the likelihood

function and the transition function simultaneously. Then, the weighted expectation–maximization (EM) algorithm is implemented to use the sampled weighted particles to generate a normal mixture model of the distribution. Unlike the Dirac-delta representation, the normal mixture model of the target-state PDF can then be easily combined with the target-dynamic equation. The computational complexity of implementing the EM algorithm is limited since the initial guess of the algorithm at a time step is the normal mixture model representation obtained in the previous time step with some disturbance.

The paper is organized as follows. Section 2 describes the target tracking and monitoring problem formulation and assumptions. The background on the particle filter and potential field methods is reviewed in Section 3. Section 4 presents the modified particle-filter information potential method. The method is demonstrated both through numerical simulations and results, presented in Section 5, and through physical experiments, presented in Section 6, conducted at the University of New Mexico's Multi-Agent, Robotics, Hybrid and Embedded Systems (MARSHES) Laboratory. Conclusions and future work are described in Section 7.

2. Problem formulation and assumptions

The problem considered in this paper consists of determining the motion and control law of a MSA, indexed by $i \in I_S$, deployed for the purpose of tracking and surveilling a moving point-mass target, indexed by $j \in I_T$, in a ROI comprising a bounded, two-dimensional Euclidian workspace $\mathcal{W} \in \mathbb{R}^2$, where I_S and I_T denote the index sets of the network of MSAs and targets, respectively. It is assumed that the assignment problem has been resolved through a multitarget–multisensor data association and assignment algorithm.[30,31] The MSA is characterized by a platform geometry $\mathcal{A}_i \in \mathbb{R}^2$, and by a bounded FOV $\mathcal{S}_i \in \mathbb{R}^2$. $\mathcal{F}_{\mathcal{A}_i}$ is a moving Cartesian frame embedded in $\mathcal{A}_i$, such that every point of $\mathcal{A}_i$ and every point of $\mathcal{S}_i$ have fixed positions with respect to $\mathcal{F}_{\mathcal{A}_i}$. Then, using a suitable transformation, the ith sensor state $\mathbf{Y}_i^\kappa = [x_i^\kappa \; y_i^\kappa \; \dot{x}_i^\kappa \; \dot{y}_i^\kappa]^{\mathrm{T}}$ can be used to specify the position and orientation of all points in $\mathcal{A}_i$ and $\mathcal{S}_j$ at t_κ, with respect to a fixed inertial frame $\mathcal{F}_\mathcal{W}$, embedded in $\mathcal{W}$. Where, x_i^κ and y_i^κ are the coordinates of the ith sensor in $\mathcal{F}_\mathcal{W}$, and $\dot{x}_i^\kappa$ and $\dot{y}_i^\kappa$ are the linear velocities in $\mathcal{F}_\mathcal{W}$, and $\mathbf{v}_i^\kappa \equiv [\dot{x}_i^\kappa, \dot{y}_i^\kappa]^{\mathrm{T}}$. Now, let ρ_{ij} denote the geometric distance between the origin of $\mathcal{F}_{\mathcal{A}_i}$ and its nearest target j in $\mathcal{W}$. Then, the objective of the ith MSA is to maintain ρ_{ij} within a predefined range,

$$\rho_0 \leq \rho_{ij} \leq \rho_1 \tag{1}$$

while avoiding a set of known, fixed, and rigid obstacles in $\mathcal{W}$, denoted by $\mathcal{B}_l$, $l \in I_B$, where I_B is an obstacle index set and ρ_0 and ρ_1 are constant parameters specified by the user.

In this paper, it is assumed that the FOV of every sensor $i \in I_S$ is a disk with radius r. The sensor dynamics are assumed to be linear and time invariant (LTI), and are discretized with respect to time, such that the sensor state transition function can be written in state-space form as

$$\mathbf{Y}_i^{\kappa+1} = \mathbf{A}\mathbf{Y}_i^\kappa + \begin{bmatrix} 0 \\ 0 \\ \delta \end{bmatrix} \mathbf{u}_i^\kappa, \quad \text{for} \quad \kappa = 0, 1, \ldots, \tag{2}$$

where κ is the time index, δ is the time span between $t^{\kappa+1}$ and t^κ, $\mathbf{u}_i \in \mathbb{R}^2$ is the control vector, $\dot{\mathbf{v}}_i^\kappa = \mathbf{u}_i^\kappa$, and

$$\mathbf{A} \equiv \begin{bmatrix} 1 & 0 & \delta & 0 \\ 0 & 1 & 0 & \delta \\ 0 & 0 & 1 & 0 \\ 0 & 0 & 0 & 1 \end{bmatrix}. \tag{3}$$

For simplicity, the sensor geometry is assumed to only translate in $\mathcal{W}$, such that the heading of the sensor is maintained constant at all times.

The motion of target $j \in I_T$ is modeled as a continuous-time Markov motion process, also known as semi-Markov jump process,[32] where we say that x_t is a *continuous-time Markov process* if for $0 \leq t_0 < \cdots < t_{k-1} < t_k < t$ we have $\Pr(x_t \in B | x_k = s_k, x_{k-1} = s_{k-1}, \ldots, x_0 = s_0) = \Pr(x_t \in B | x_k = s_k)$. Here Pr denotes the probability transition function, and $s_1, \ldots, s_k \in \mathcal{X}$ are realizations of the state space $\mathcal{X}$. Now, let the random variables θ_j^k and v_j^k represent the jth target's heading and velocity, respectively, during the time interval $\Delta t_k = (t_{k+1} - t_k)$, $k = 1, 2, \ldots$. Then, the target motion can be modeled as a continuous-time Markov process with a family of random variables $\{\mathbf{x}_j^k, \theta_j^k, v_j^k\}$, where $\mathbf{x}_j^k \in \mathcal{W}$ is the jth target position at t_k. A three-dimensional real-valued vector function maps the family of random variables $\{\theta_j^k, v_j^k\}$ into the random vector $\mathbf{x}_j(t)$, such that the value of the target motion process is given by

$$\dot{\mathbf{x}}_j(t) = v_j(t)[\cos\theta_j(t) \quad \sin\theta_j(t)]^{\mathrm{T}}, \tag{4}$$

and, therefore, the motion of target j is a Markov process. The third component of the vector function is the identity function. It follows that θ_j and v_j are piecewise constant, while $\mathbf{x}_j$ has discontinuities at the time instants t_k, when the target j changes its heading and velocity. In this paper, it is assumed that the instants when the target changes its heading are known *a priori*, and all targets move at a constant speed $v_j = v$. Also, it assumed that all time intervals are of constant length, i.e. $\Delta t_k = \tau$, for $\forall k$.

Now, let $\mathbf{X}_j^k = [\mathbf{x}_j^k \; \theta_j^k]^{\mathrm{T}}$ denote the jth target state at time step k. The probability transition function for the target heading at the instant t_k of a discontinuity, is defined as

$$f(\theta_j^{k+1},|\,\theta_j^k)=\mathcal{N}(\theta_j^{k+1}|\;\mu+\theta_j^k,\sigma^2) \tag{5}$$

where the mean of heading change μ and the variance of the heading change σ are constant parameters that are assumed known *a priori*. The target heading remains constant during every time interval Δt_k, The target state transition function at every discontinuity is given by

$$\mathbf{X}_i^{k+1}=\mathbf{X}_j^k+\begin{bmatrix}\cos(\theta_j^k)\tau v\\ \sin(\theta_j^k)\tau v\\ \mathcal{N}(\mu,\sigma^2)\end{bmatrix},\quad \text{for}\quad \forall k. \tag{6}$$

where τ is the known length of the time interval Δt_k.

The MSAs attempt to obtain measurements of the targets' positions once with a frequency of $1/\delta$ (Hz), where $\delta<\tau$. Thus, if at time instant t_κ, the *j*th target is inside the *i*th sensor's FOV, then the *i*th MSA can obtain a measurement of the *j*th target position,

$$\mathbf{z}_i^\kappa=\mathbf{x}_j^\kappa+v_{ij}\Leftarrow\mathbf{x}_j(t_\kappa)\in\mathcal{S}_i \tag{7}$$

where $\mathbf{x}_j^\kappa$ is the *j*th target's position at time t_κ, and v_{ij} is a white-noise error with standard deviation Σ_{ij}. If $\mathbf{x}_j(t_\kappa)\notin\mathcal{S}_i$, no measurements are returned to the *i*th sensor.

3. Background

3.1 Particle filter methods

The particle filter technique is a recursive model estimation method based on sequential Monte Carlo simulations. It is applicable to nonlinear system dynamics with non-Gaussian random inputs. Moreover, because of their recursive nature, particle filters are easily applicable to online data processing and variable estimation. The main idea of particle filters is to represent the PDF functions with properly weighted and relocated point masses, known as particles. These particles are sampled from an importance density which is crucial to the particle filter algorithm. Let $\{\mathbf{x}_{j,p}^\kappa,w_{j,p}^\kappa\}_{p=1}^N$ denote the weighted particles that are used to approximate the posterior PDF $f(\mathbf{x}_j^\kappa\,|\,Z_j^\kappa)$ for the *j*th target at t_κ, where $Z_j^\kappa=\{\mathbf{z}_j^0,\ldots,\mathbf{z}_j^\kappa\}$ denotes the set of all measurements obtained by sensor *i*, from target *j*, up to t_κ. Then, the posterior PDF of the target state, given the measurement at t_κ can be modeled as,

$$f(\mathbf{x}_j^\kappa\,|\,Z_j^\kappa)=\sum_{p=1}^N w_{j,p}^\kappa\delta(\mathbf{x}_{j,p}^\kappa),\qquad\sum_{p=1}^N w_{j,p}^\kappa=1 \tag{8}$$

where $w_{j,p}^\kappa$ is non-negative and δ is the Dirac delta function.[24] Although different particle filter techniques have been proposed,[26] the techniques always consist of the recursive propagation of the particles and the particle weights. In each iteration, the particles $\mathbf{x}_{j,p}^\kappa$ are sampled from the importance density $q(\mathbf{x})$. Then, weight $w_{j,p}^k$ is updated for each particle by

$$w_{j,p}^\kappa\propto\frac{p(\mathbf{x}_{j,p}^\kappa)}{q(\mathbf{x}_{j,p}^\kappa)} \tag{9}$$

where $p(\mathbf{x}_{j,p}^\kappa)\propto f(\mathbf{x}_{j,p}^\kappa\,|\,Z_j^\kappa)$. In addition, the weights are normalized at the end of each iteration.

Since the target state transition function is often used as the importance density function without considering the available new measurement, the sampled particles can not fully represent the target state estimation. Another common drawback of particle filters is the degeneracy phenomenon,[28] i.e. the variance of particle weights accumulates along iterations. This phenomenon indicates that a number of particles have low weights and no contributions in approximating the probability density function $f(\mathbf{x}_j^\kappa\,|\,\mathbf{z}_j^\kappa)$ but put heavy computational burden to the algorithm. The number of particles with high weights is not sufficient to provide a good approximation. A common way to evaluate the degeneracy phenomenon is the effective sample size N_e,[27] obtained by

$$N_e=\frac{1}{\sum_{p=1}^N(w_{j,p}^\kappa)^2} \tag{10}$$

where $w_{j,p}^\kappa,p=1,2,\ldots,N$ are the normalized weights. In general, a re-sampling procedure is taken when $N_e<N_s$, where N_s is a predefined threshold, and is usually set as $\frac{N}{2}$. Let $\{\mathbf{x}_{j,p}^\kappa,w_{j,p}^\kappa\}_{p=1}^N$ denote the particle set that needs to be re-sampled, and let $\{\mathbf{x}_{j,p}^{\kappa*},w_{j,p}^{\kappa*}\}_{p=1}^N$ denote the particle set after re-sampling. The main idea of this re-sampling procedure is to eliminate the particles having low weights by re-sampling $\{\mathbf{x}_{j,p}^{\kappa*},w_{j,p}^{\kappa*}\}_{p=1}^N$ from $\{\mathbf{x}_{j,p}^\kappa,w_{j,p}^\kappa\}_{p=1}^N$ with the probability of $p(\mathbf{x}_{j,p}^{\kappa*}=\mathbf{x}_{j,s}^\kappa)=w_{j,s}^\kappa$. At the end of the resampling procedure, $w_{j,p}^{\kappa*},p=1,2,\ldots,N$ are set as $1/N$. However, the resampling procedure repeats the particles with high weights a number of times stochastically. This leads to diversity loss of particles.

In this paper, a modified particle filter approach with a new sampling method based on supporting intervals of PDFs is proposed. The advantage of the proposed sampling method is that the latest measurement by sensors is taken into account when particles are sampled. As a result, the sampled particles can more efficiently approximate the estimation. Moreover, a mixture Gaussian is used to represent the PDF of the target state instead of a set of properly weighted and located point-mass approximations by Dirac delta functions in order to avoid the degeneracy phenomenon.

3.2 Potential Field

The potential field method is a robot path planning technique that uses an artificial potential function to find the obstacle-free path in an Euclidean workspace. The geometries and positions of the obstacles and targets are considered as sources to construct a potential function U which represents the characteristics of the workspace. Although different approaches have been proposed to generate the potential function based on obstacles' geometries[33–35], typically the potential function consists of two components, the repulsive potential U_{rep} generated by the obstacles,[36] and the attractive potential U_{att} generated by the robot goal configuration

$$U(\mathbf{q}) = U_{att}(\mathbf{q}) + U_{rep}(\mathbf{q}), \tag{11}$$

where $\mathbf{q} = [x\ y\ \theta]^{\mathrm{T}}$ is the robot configuration in $\mathcal{W}$, which specifies the robot's position (x and y coordinates) and orientation (θ) with respect to $\mathcal{F}_{\mathcal{W}}$.[36] Recently, an information potential approach was developed for generating an attractive potential based on target geometries and information value in sensor path planning problems, such as the treasure hunt.[7] Once the potential is generated, a virtual force is applied on the robot that is proportional to the negative gradient of U, and can be implemented through a suitable control law, such that U constitutes a Lyapunov function that may be utilized to prove closed-loop stability.

For a robot with a finite platform geometry $\mathcal{A}$, the potential field is generated by taking into consideration the robot configuration space $\mathcal{C}$, and the corresponding obstacles' geometries $\mathcal{B}$. A C-obstacle is defined as the subset of $\mathcal{C}$ that causes collisions with at least one obstacle in $\mathcal{W}$, i.e. $\mathcal{CB}_l \equiv \{\mathbf{q} \in \mathcal{C} \mid \mathcal{A}(\mathbf{q}) \cap \mathcal{B}_l \neq \varnothing\}$, where $\mathcal{A}(\mathbf{q})$ denotes the subset of $\mathcal{W}$ occupied by the platform geometry $\mathcal{A}$ when the robot is at the configuration $\mathbf{q}$. The union of all C-obstacles in $\mathcal{W}$ is referred to as the C-obstacle region. Thus, in searching for targets in $\mathcal{W}$, the robotic sensor is free to rotate and translate in the free configuration space, which is defined as the complement of the C-obstacle region $\mathcal{CB}$ in $\mathcal{C}$, i.e. $\mathcal{C}_{free} = \mathcal{C} \backslash \mathcal{CB}$.[36]

Then, the repulsive potential can be represented as

$$U_{rep}(\mathbf{q}) = \begin{cases} \frac{1}{2}\eta\left(\frac{1}{\rho(\mathbf{q})} - \frac{1}{\rho_0}\right)^2 & \text{if} \quad \rho(\mathbf{q}) \leq \rho_0 \\ 0 & \text{if} \quad \rho(\mathbf{q}) > \rho_0 \end{cases} \tag{12}$$

where η is a scaling factor, $\rho(\mathbf{q})$ is the distance between the robot and the nearest obstacle in Euclidean space, and ρ_0 is a constant parameter that is chosen by the user. The attractive potential is given by

$$U_{att}(\mathbf{q}) = \frac{1}{2}\varepsilon\rho_{goal}^2(\mathbf{q}), \tag{13}$$

where ε is a scaling factor, and $\rho_{goal}(\mathbf{q})$ is the distance between the robot and the goal configuration. In (12) and (13), only the obstacle closest to $\mathbf{q}$ is considered to generate $U_{rep}(\mathbf{q})$, and the target is assumed to be a single point in $\mathcal{C}_{free}$. This makes the potential function difficult to update when new obstacles and targets are sensed during the path execution, because for each value of $\mathbf{q}$, the potential needs to update by computing its distance from the closest obstacle and target. The next section presents a modified potential function that takes the target Markov properties into account in order to minimize the distance traveled by the MSA.

4. Methodology

The information potential method presented in this paper can be used to compute the path plan and control law for a MSA that must monitor a moving target, based on the tracking information provided by a modified particle filter. For simplicity, it is assumed that the target velocity is known and constant, and the time instants at which the discontinuities take place are known and occur at constant intervals. However, the methodology can be generalized, and these assumptions relaxed, by computing the PDFs of all Markov parameters using the proposed particle filter. Here, the particle filter technique is used to obtain the PDF of the target heading, and to update it with every new measurement $\mathbf{z}_j^{\kappa}$ over time. In the proposed method, a finite normal mixture is utilized to represent the PDF of the target heading,

$$f(\theta) = \sum_{\ell=1}^{m} \pi_\ell \mathcal{N}(\theta \mid \mu_\ell, \sigma_\ell^2), \qquad \sum_{\ell=1}^{m} \pi_\ell = 1,\ \pi_\ell \geq 0\ \forall \ell, \tag{14}$$

where $f(\cdot)$ is used to denote a PDF of the arguments in parenthesis, m is the number of normal components, which is assigned a user-defined upper limit M. Here μ_ℓ and σ_ℓ are the mean and variance for ℓth normal component. Prior to obtaining target measurements, the number of components is set to $m = M$, μ_ℓ is uniformly sampled from the interval $[-\pi\ \pi]$, and σ_ℓ is chosen equal to a user-defined value σ_0. Let $\mathbf{z}_j^{\kappa}$ denote the measurement obtained by sensor i at t^{κ}, as shown in (7). Then, the PDF of the jth target's heading at t_{κ}, based on the set Z_j^{κ}, modeled by the finite normal mixture,

$$f(\theta_j^{\kappa} \mid Z_j^{\kappa}) \leftarrow \sum_{\ell=1}^{m} \pi_{j,\ell}^{\kappa} \mathcal{N}(\theta_j^{\kappa} \mid \mu_{j,\ell}^{\kappa}, (\sigma_{j,\ell}^{\kappa})^2) \tag{15}$$

is updated based on the target transition probability function (5). Since the change in the target state is characterized by a Gaussian distribution,

$$\theta_j^{\kappa+1} - \theta_j^k \sim \mathcal{N}(\mu, \sigma^2) \tag{16}$$

the distribution of $\theta_j^{\kappa+1}$ given Z_j^κ, and irrespective of $\mathbf{z}_j^{\kappa+1}$, is given by

$$\begin{aligned}\theta_j^{\kappa+1} \mid Z_j^\kappa &\sim \mathcal{N}(\mu, \sigma^2) + \sum_{\ell=1}^{m} \pi_{j,\ell}^\kappa \mathcal{N}(\mu_{j,\ell}^\kappa, (\sigma_{j,\ell}^\kappa)^2) \\ &\sim \sum_{\ell=1}^{m} \pi_{j,\ell}^\kappa (\mathcal{N}(\mu, \sigma^2) + \mathcal{N}(\mu_{j,\ell}^\kappa, (\sigma_{j,\ell}^\kappa)^2)) \\ &\sim \sum_{\ell=1}^{m} \pi_{j,\ell}^\kappa \mathcal{N}(\mu_{j,\ell}^\kappa + \mu, (\sigma_{j,\ell}^\kappa)^2 + \sigma^2)\end{aligned} \tag{17}$$

and the PDF of the target heading at $t_{\kappa+1}$ is given by

$$f(\theta_j^{\kappa+1} \mid Z_j^\kappa) = \sum_{\ell=1}^{m} \pi_{j,\ell}^\kappa \mathcal{N}(\theta_j^{\kappa+1} \mid \mu_{j,\ell}^\kappa + \mu, (\sigma_{j,\ell}^\kappa)^2 + \sigma^2). \tag{18}$$

Bayes' rule is used to compute $f(\theta_j^{\kappa+1} \mid Z_j^{\kappa+1})$ based on $\mathbf{z}_j^{\kappa+1}$ and $f(\theta_j^{\kappa+1} \mid Z_j^\kappa)$, as follows,

$$\begin{aligned}f(\theta_j^{\kappa+1} \mid Z_j^{\kappa+1}) &\leftarrow f(\theta_j^{\kappa+1} \mid \mathbf{z}_j^{\kappa+1}, Z_j^\kappa) \\ &= \frac{f(\mathbf{z}_j^{\kappa+1} \mid \theta_j^{\kappa+1}, Z_j^\kappa) f(\theta_j^{\kappa+1} \mid Z_j^\kappa)}{f(\mathbf{z}_j^{\kappa+1} \mid Z_j^\kappa)} \\ &\propto f(\mathbf{z}_j^{\kappa+1} \mid \theta_j^{\kappa+1}, Z_j^\kappa) f(\theta_j^{\kappa+1} \mid Z_j^\kappa),\end{aligned} \tag{19}$$

where $f(\mathbf{z}_j^{\kappa+1} \mid \theta_j^{\kappa+1}, Z_j^\kappa)$ is determined from the measurement model,

$$\begin{aligned}f(\mathbf{z}_j^{\kappa+1} \mid \theta_j^{\kappa+1}, Z_j^\kappa) &\approx f(\mathbf{z}_j^{\kappa+1} \mid \theta_j^{\kappa+1}, \tilde{\mathbf{x}}_j^\kappa) \\ &= \frac{1}{\sqrt{2\pi} \parallel \sum_j \parallel} \exp\left(- \frac{\parallel \mathbf{z}_j^\kappa - \tilde{\mathbf{x}}_j^\kappa - \delta v \begin{bmatrix} \cos(\theta_j^{\kappa+1}) \\ \sin(\theta_j^{\kappa+1}) \end{bmatrix} \parallel^2}{2 \parallel \sum_j \parallel^2} \right),\end{aligned}$$

where $\sum_j$ is the covariance, v is the target linear velocity, and $\tilde{\mathbf{x}}_j^\kappa$ is the target position estimation obtained at t^κ. The modified particle filter is used to evaluate equation (19), where the importance density function is based on the supporting intervals of distributions. The PDFs $f(\mathbf{z}_j^\kappa \mid \theta_j^{\kappa+1}, Z_j^\kappa)$ and $f(\theta_j^{\kappa+1} \mid Z_j^\kappa)$ are both considered as distributions of $\theta_j^{\kappa+1}$. Let S denote the support interval for a PDF $f(x)$, and R denote the definitive range for $f(x)$. Then, the support interval S of $f(x)$ is defined as $f(x) > \gamma, \forall x \in S$. Now, let S_j^m denote the support interval of $f(\mathbf{z}_j^\kappa \mid \theta_j^{\kappa+1}, Z_j^\kappa)$ and S_j^p denote the support interval of $f(\theta_j^{\kappa+1} \mid Z_j^\kappa)$. It follows that $S = S_j^m \cup S_j^p$, where, the importance density function for sampling particles is defined as

$$f(\theta_j^{\kappa+1}) = \begin{cases} \frac{1}{L} & \text{if } \theta_j^{\kappa+1} \in S \\ 0 & \text{otherwise} \end{cases} \tag{20}$$

and

$$L = \int_R g(\theta_j^{\kappa+1}) d\theta_j^{\kappa+1}, \qquad g(\theta_j^{\kappa+1}) = \begin{cases} 1 & \text{if } \theta_j^{\kappa+1} \in S \\ 0 & \text{otherwise.} \end{cases} \tag{21}$$

The weight for each particle is obtained by mixing the previous target state estimation and the target state likelihood function together simultaneously. By considering $f(\mathbf{z}_j^{\kappa+1} \mid \theta_j^{\kappa+1}, Z_j^\kappa)$ and $f(\theta_j^{\kappa+1} \mid Z_j^\kappa)$, the weight $w_{j,p}^{\kappa+1}$ for pth particle of jth target, denoted as $\theta_{j,p}^{\kappa+1}$, is updated as follows:

$$w_{j,p}^{\kappa+1} = f(\mathbf{z}_{j,p}^{\kappa+1} \mid \theta_{j,p}^{\kappa+1}, Z_j^\kappa) f(\theta_{j,p}^{\kappa+1} \mid Z_j^\kappa). \tag{22}$$

The weight for each particle is normalized using the equation

$$w_{j,p}^{\kappa+1} = \frac{w_{j,p}^{\kappa+1}}{\sum_{p=1}^{N} w_{j,p}^{\kappa+1}} \tag{23}$$

and the weighted EM algorithm, shown in Table 1, is implemented to obtain a normal mixture representation of the target heading's PDF, using weighted particles. After the target heading is obtained, the target position is estimated based on the sensor measurement obtained during the latest time interval, using the least-squares error method.

In order to maintain the distance ρ_{ij}, between sensor i and target j, within the desired range (1), a new potential function is proposed as follows. We seek a function U of the MSA configuration, such that when ρ_{ij} is less than a positive threshold ρ_0, U becomes a repulsive potential, and when ρ_{ij} is greater than a positive threshold ρ_1, U becomes an attractive potential. Let $\mathbf{q}_i^\kappa$ denote the configuration of sensor i, and $\mathbf{q}_j^\kappa$ denote the configuration of target j at t_κ. Without considering the knowledge of the targets' Markov property, the potential function for the ith sensor at time t_κ is defined as

$$U_e(\mathbf{q}_i^\kappa) \equiv \begin{cases} \frac{1}{2}\eta\left(\frac{1}{\rho(\mathbf{q}_j^\kappa, \mathbf{q}_i^\kappa)} - \frac{1}{\rho_0}\right)^2, & \text{if } \rho(\mathbf{q}_j^\kappa, \mathbf{q}_i^\kappa) \le \rho_0 \\ 0, & \text{if } \rho_0 < \rho(\mathbf{q}_j^\kappa, \mathbf{q}_i^\kappa) < \rho_1 \\ \frac{1}{2}\xi(\rho(\mathbf{q}_j^\kappa, \mathbf{q}_i^\kappa) - \rho_1)^2, & \text{if } \rho(\mathbf{q}_j^\kappa, \mathbf{q}_i^\kappa) \ge \rho_1 \end{cases} \tag{24}$$

and its potential field is referred to as the 'exact potential field'. In order to minimize the MSA's traveling distance, the target heading at the next time interval, denoted by θ^{k+1}, is also considered in the definition of the novel

Table 1. Weighted EM algorithm.

Initialize $\sum_{\ell=1}^{M} \pi_{j,\ell}^{\kappa+1}\mathcal{N}(\mu_{j,\ell}^{\kappa+1},\sigma_{j,\ell}^{\kappa+1})$ as $\sum_{\ell=1}^{M} \pi_{j,\ell}^{\kappa}\mathcal{N}(\mu_{j,\ell}^{\kappa},\sigma_{j,\ell}^{\kappa})$
Iterate until $\sum_{\ell=1}^{M} \pi_{j,\ell}^{\kappa+1}\mathcal{N}(\mu_{j,\ell}^{\kappa+1},\sigma_{j,\ell}^{\kappa+1})$ converges
  for each particle p
    $f_{p,\ell} = \pi_{j,\ell}^{\kappa+1}\mathcal{N}(\theta_{j,p}^{\kappa+1} \mid \mu_{j,\ell}^{\kappa+1},\sigma_{j,\ell}^{\kappa+1})$
    cluster pth particle into group G_l if $f_{p,\ell} \geq f_{p,r\neq\ell}$
  end
  for each group ℓ
    $\mu_{j,\ell}^{\kappa+1} = \frac{\sum w_{j,p}^{\kappa+1}\theta_{j,p}^{\kappa+1}}{\sum w_{j,p}^{\kappa+1}}, \theta_{j,p}^{\kappa+1} \in G_\ell$
    $\sigma_{j,\ell}^{\kappa+1} = \frac{\sum w_{j,p}^{\kappa+1}(\theta_{j,p}^{\kappa+1}-\mu_{j,\ell}^{\kappa+1})^2}{\sum w_{j,p}}, \theta_{j,p}^{\kappa+1} \in G_\ell$
    $\pi_{j,\ell}^{\kappa+1} = \sum w_{j,p}^{\kappa+1}, \theta_{j,p}^{\kappa+1} \in G_\ell$
  end
  if $\pi_{j,\ell}^{\kappa+1} \leq \zeta$
    set $\pi_{j,\ell}^{\kappa+1} = 0$
  end
end

potential function. The expected value of θ^{k+1}, denoted by $\tilde{\theta}^{k+1}$, is obtained from (5)

$$\tilde{\theta}_j^{\,k+1} = \mathbb{E}\{\theta_j^{k+1}\} = \sum_{\ell=1}^{m} \pi_{j,\ell}^{\kappa}\theta_{j,\ell}^{\kappa} + \mu \tag{25}$$

Then, a potential function that takes into account the target motion can be defined as follows

$$U^*(\mathbf{q}_i^{\kappa}) \equiv \begin{cases} \frac{1}{2}\eta\left(\frac{1}{\rho(\mathbf{q}_j^{\kappa},\mathbf{q}_i^{\kappa})} - \frac{1}{\rho_0}\right)^2, & \text{if } \rho(\mathbf{q}_j^{\kappa},\mathbf{q}_i^{\kappa}) \leq \rho_0 \\ 0, & \text{if } \rho_0 < \rho(\mathbf{q}_j^{\kappa},\mathbf{q}_i^{\kappa}) < \rho_1 \\ \frac{1}{2}\xi(\rho(\mathbf{q}_j^{\kappa *},\mathbf{q}_i^{\kappa}) - \rho_1)^2, & \text{if } \rho(\mathbf{q}_j^{\kappa},\mathbf{q}_i^{\kappa}) \geq \rho_1, \end{cases} \tag{26}$$

where

$$\mathbf{q}_j^{\kappa *} = \mathbf{q}_j^{\kappa} + \alpha \begin{bmatrix} \cos\tilde{\theta}_j^{k+1} \\ \sin\tilde{\theta}_j^{k+1} \end{bmatrix} [\rho(\mathbf{q}_j^{\kappa},\mathbf{q}_i^{\kappa}) - \rho_1] \tag{27}$$

and the parameter α is a positive constant defined by the user. The potential field in (26) is referred to as the 'virtual potential field'.

When the distance between the sensor and the target is within the predefined interval, the virtual potential field (26) converges to the exact potential field (24), i.e. $U^*(\mathbf{q}_i^{\kappa}) = U(\mathbf{q}_i^{\kappa})$. The artificial force is provided by the negative gradient of $U^*(\mathbf{q}_i^{\kappa})$,

$$\mathbf{F}(\mathbf{q}_i^{\kappa}) = -\nabla U^*(\mathbf{q}_i^{\kappa}), \tag{28}$$

or, from (26),

$$F(\mathbf{q}_i^{\kappa}) = \begin{cases} \eta\left(\frac{1}{\rho(\mathbf{q}_j^{\kappa},\mathbf{q}_i^{\kappa})} - \frac{1}{\rho_0}\right)\frac{\nabla\rho(\mathbf{q}^{\kappa},\mathbf{q}_i^{\kappa})}{\rho^2(\mathbf{q}^{\kappa},\mathbf{q}_i^{\kappa})}, & \text{if } \rho(\mathbf{q}_j^{\kappa},\mathbf{q}_i^{\kappa}) \leq \rho_0 \\ 0, & \text{if } \rho_0 < \rho(\mathbf{q}_j^{\kappa},\mathbf{q}_i^{\kappa}) < \rho_1. \\ -\xi(\rho(\mathbf{q}^{\kappa *},\mathbf{q}_i^{\kappa}) - \rho_1)\nabla\rho(\mathbf{q}^{\kappa *},\mathbf{q}_i^{\kappa}), & \text{if } \rho(\mathbf{q}_j^{\kappa},\mathbf{q}_i^{\kappa}) \geq \rho_1 \end{cases} \tag{29}$$

Then, as in classical potential field methods,[37,38] the feedback control law for the MSA can be formulated as a function of the artificial force, i.e.

$$\mathbf{u}(\mathbf{q}_i^{\kappa}) = (\dot{\mathbf{x}}_j^{\kappa} - \mathbf{v}_i^{\kappa}) + F(\mathbf{q}_i^{\kappa}). \tag{30}$$

In order to guarantee closed-loop stability for the feedback control law (30), the Lyapunov function,

$$V = \frac{1}{2}(\dot{\mathbf{x}}_j^{\kappa} - \mathbf{v}_i^{\kappa})^{\mathrm{T}}(\dot{\mathbf{x}}_j^{\kappa} - \mathbf{v}_i^{\kappa}) + U^*(\mathbf{q}_i^{\kappa}) \tag{31}$$

From (2), (30), and (31), the time derivative of the Lyapunov function in (31) is

$$\begin{aligned} \dot{V} &= (\dot{\mathbf{x}}_j^{\kappa} - \mathbf{v}_i^{\kappa})(-\dot{\mathbf{v}}_i^{\kappa}) - \nabla U^*(\mathbf{q}_i^{\kappa})(\dot{\mathbf{x}}_j^{\kappa} - \mathbf{v}_i^{\kappa}) \\ &= (\dot{\mathbf{x}}_j^{\kappa} - \mathbf{v}_i^{\kappa})(-(\dot{\mathbf{x}}_j^{\kappa} - \mathbf{v}_i^{\kappa}) + \nabla U^*(\mathbf{q}_i^{\kappa})) \\ &\quad - \nabla U^*(\mathbf{q}_i^{\kappa})(\dot{\mathbf{x}}_j^{\kappa} - \mathbf{v}_i^{\kappa}) = -(\dot{\mathbf{x}}_j^{\kappa} - \mathbf{v}_i^{\kappa})^{\mathrm{T}}(\dot{\mathbf{x}}_j^{\kappa} - \mathbf{v}_i^{\kappa}) \leq 0. \end{aligned} \tag{32}$$

Furthermore, $V \geq 0$ because $U^*(\mathbf{q}_i^{\kappa}) \geq 0$. It follows from the Lyapunov stability theorem[39] that the MSA control law in (30) is asymptotically stable, $U^*(\mathbf{q}_i^{\kappa}) \to 0$, and ρ_{ij} converges to a value within $[\rho_0\ \rho_1]$.

5. Numerical simulations and results

The effectiveness of the particle-filter information potential method is demonstrated through two scenarios simulated numerically in Matlab®.[40] One scenario is used to test the modified particle filter presented in Section 4, and assumes that the sensor and the target can be modeled as point masses. Another scenario considers the geometries of the MSA, target, and obstacles in the workspace. In the first scenario, the workspace is an obstacle-free ROI with dimensions 50 [m] × 50 [m]. A single target that changes its heading every 10 [s], maneuvers in the ROI at a constant speed of 2 [m/s]. The MSA's omnidirectional FOV is chosen to have a radius of 10 [m]. Within the FOV, the sensor obtains measurements of the target position every 0.3 [s], according to the model in (7), and with a standard deviation $\Sigma = \mathrm{diag}(0.4, 0.4)$. The effectiveness of the modified particle filter is determined based on the estimation error of the target heading

$$\varepsilon = \tilde{\theta}^{\kappa} - \theta^{\kappa}, \tag{33}$$

where $\tilde{\theta}^{\kappa}$ is the estimated target heading estimation, and θ^{κ} is the actual target heading.

A plot of the estimation error associated with first scenario is shown in Figure 1. It can be seen that, at the initial time, the estimated target heading varies greatly from the actual target heading, because no prior target information is available. Once target detections are obtained, however, the estimation error quickly converges to zero, until the target maneuvers at times $k = 1$, and $k = 2$. As shown in Figure 1, at these times the estimation error grows significantly because the target suddenly changes direction. As the sensor obtains new target measurements over time, the estimation error, once again, goes back to zero. These simulations illustrate the effectiveness of the modified particle filter in estimating the target heading from available sensor measurements.

The particle-filter information potential method is demonstrated through a second scenario involving one target with geometry $\mathcal{T}$, seven obstacles with geometries $\mathcal{B}_l$, $l = 1, \ldots, 7$, and an omnidirectional MSA with FOV $\mathcal{S}$, all shown in Figure 2. The workspace is a ROI with dimensions 100 [m] $\times$ 10 [m], populated with obstacles modeled as convex polygons. The MSA is considered to successfully monitor the target when, from (1), it can maintain a distance ρ_{ij} from the target, where $3\ [\text{m}] < \rho_{ij} < 4\ [\text{m}]$, while simultaneously avoiding collisions with the obstacles. The results, plotted in Figures 2 and 3, show that the path of the MSA allows the sensor to successfully monitor the target even when the target maneuvers and momentarily exists the MSA's FOV.

As shown by a plot of the Euclidean distance between the sensor and the target, in Figure 3, when the target maneuvers, as indicated by the vertical dashed lines (Figure 3), ρ_{ij} exceeds its bounds for a short period of time. Subsequently, through the modified particle filter output, the information potential control law (30) forces ρ_{ij} to within the required range, such that the MSA can continue obtaining measurements from the target, while remaining at a minimum distance of 3 [m] from it. Furthermore, the modified particle filter is capable of estimating target heading even in the presence of non-Gaussian sensor noise.

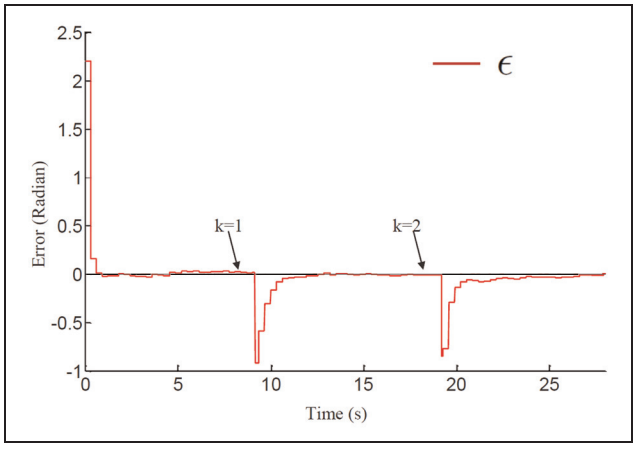

Figure 1. Target heading estimation.

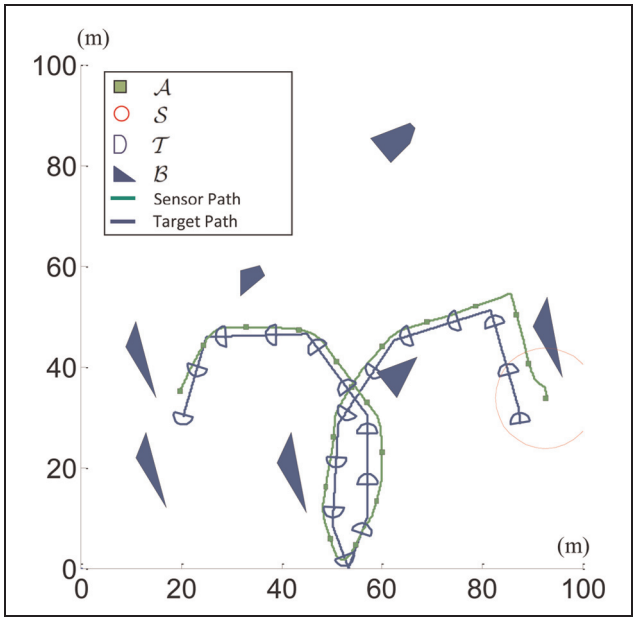

Figure 2. MSA and target path in an obstacle-populated ROI.

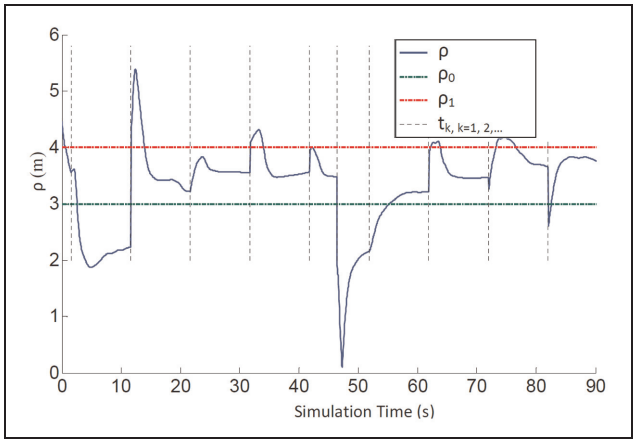

Figure 3. Time history of the Euclidian distance between sensor *i* and target *j*.

6. Physical experiments

6.1 Experimental setup

A physical experiment demonstrating preliminary results for the scenario in Figure 1, and testing various aspects of the methodology presented in this paper, was conducted at

Figure 4. Left to right: Tamiya TXT-1, AscTec Quadrotor, and MARHES flight cage.

the University of New Mexico's MARHES Laboratory. The experiment was conducted using the MARHES Robotic Test Bed (Figure 4), consisting of an AscTec Quadrotor UAV and a custom robotic hybrid electric vehicle test bed, which is based on a hobbyist RC truck chassis known as the Tamiya TXT-1. The quadrotor was employed in the experiment as the sensing agent, and the TXT-1 was used as the target. The target vehicle is controlled using a custom low-level controller designed in ROS (Robotic Operating System from Willow Garage) to feed linear and angular velocity commands from a joystick, and was driven in the experiment by a human operator. The quadrotor is controlled using a custom LabVIEW controller via a National Instruments CompactRio, a real-time control board with commands and telemetry being transmitted wirelessly from the CompactRio control station to the quadrotor via a Zigbee wireless transceiver pair. This 'low-level' control for the quadrotor accepts (x, y) reference point commands and controls the quadrotor to move to and maintain a hover state at such a waypoint or set point.

A Vicon Motion Capture System provides position data accurately to within 3 [mm], and the data is obtained with a frequency of around 300 [Hz]. This Vicon data is used both in the low-level controller for the quadrotor for positioning data for feedback control, and in the artificial simulated sensor for the sensing agent that is used to measure target states and detect possible obstacles. The high-level sensing agent control for conducting the target tracking experiment was written in Matlab and embedded in LabVIEW. The artificial sensor and particle filter for estimating target motion, the calculation of potential gradients, and the position set point control were embedded in Matlab Script Nodes in LabVIEW. The workspace where the experiment was being conducted consisted of an obstacle-free ROI of approximately 3 [m] $\times$ 4 [m], enclosed by a safety net and observed by the Vicon Motion Capture System. The small size of the workspace necessitated the choice of a small desired monitoring ring of about 0.2 [m] from the target. In this case, target and sensor were allowed to occupy the same position as they are at different altitudes. Therefore, the monitoring bound in (1) was given by $0 < \rho_{ij} < 0.2$ [m]. As in previous sections, the target velocity was assumed known and constant.

6.2 Experimental results

The preliminary experiments showed that the quadrotor was able to successfully monitor the target using the algorithm described in Section 4. Figure 5 shows that when the MSA is initially deployed to follow the calculated set point from the control algorithm, and while the target is stationary, the MSA moves to a position near the target, and within the desired 0.2 [m] for target monitoring. Once the target begins moving, in Figures 6–8, it can be seen that the MSA infers the target position (from the target heading) within reasonable accuracy, and moves to continue monitoring the target over time. Delays were

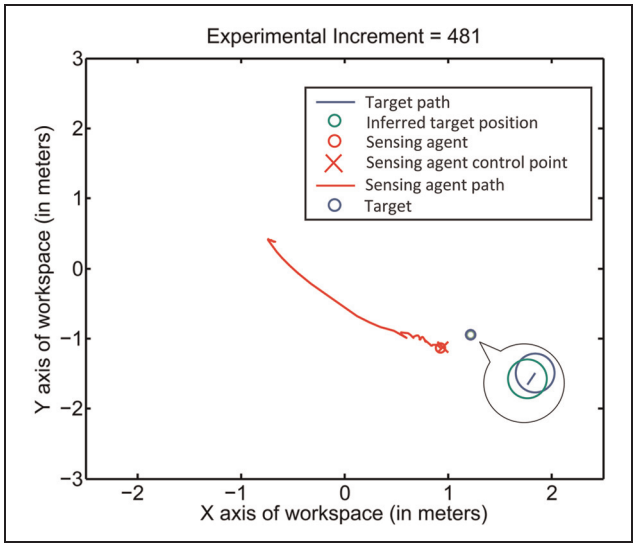

Figure 5. Sensing agent control enabled.

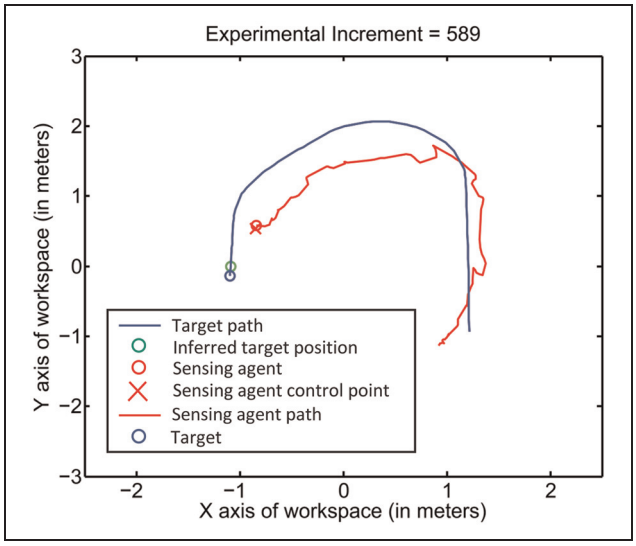

Figure 6. Target motion segment 1.

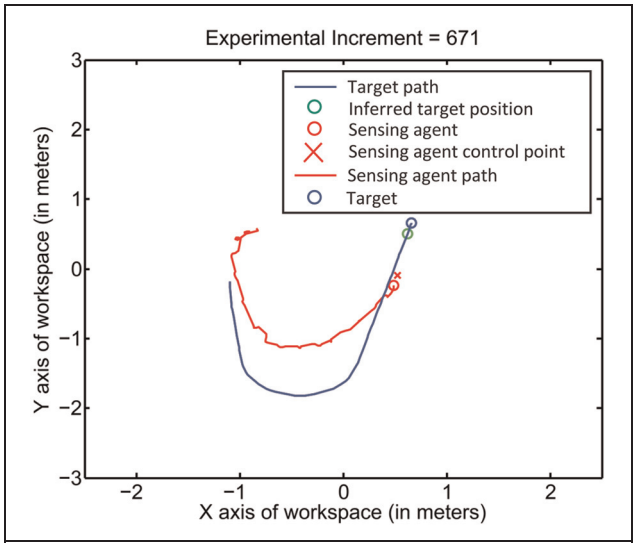

Figure 7. Target motion segment 2.

observed in these initial experiments that we attributed to timing and communication constraints between Matlab and LabVIEW. In addition, the distance between target and the MSA is at times greater than 0.2 [m]. This was attributed to a need for more precise tuning of the particle filter parameters and the potential gradient generation.

7. Summary and conclusions

This paper presents an information potential approach for computing MSA's motion plans and control inputs based on the feedback from a modified particle filter used for tracking a maneuvering target, based on little or no prior information. The modified particle filter presented in this paper implements a new sampling method, based on supporting intervals of density functions. The filter accounts for the latest sensor measurements, by adapting a normal mixture representation of the probability density functions associated with the target motion. In this modified particle filter, the importance density of the particles is a function of the latest measurements' probability distribution, and of the probability distribution at the previous time step. A new information potential method for Markov target motion models is developed to accomplish the MSA objective of monitoring the maneuvering target, while minimizing the distance traveled, and avoiding collisions with potential obstacles. The results of numerical and physical simulations demonstrate that the modified particle filter is capable of estimating the target heading, using the proposed supporting interval sampling method and Gaussian mixture approach. Also, they demonstrate that the MSA is capable of monitoring the target over time, even in the presence of sharp maneuvers, and in the absence of an accurate target motion model.

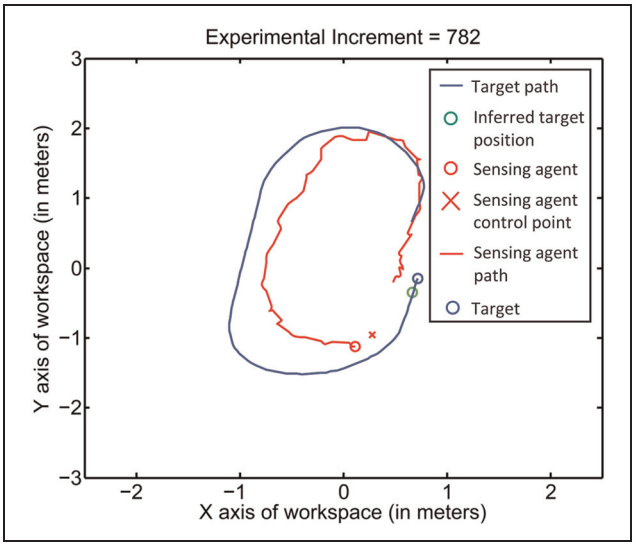

Figure 8. Target motion segment 3.

Acknowledgment

Special thanks to Patricio J Cruz and Titus Appel, fellow students at UNM MARHES laboratory, for their help in conducting the hardware experiment.

Funding

This work was supported by the NSF (grant numbers ECCS #1027775, and ECCS #1028506), and by the

Department of Energy (URPR grant #DE-FG52-04NA25590).

References

1. Ferrari S, Cai C, Fierro R and Perteet B. A multi-objective optimization approach to detecting and tracking dynamic targets in pursuit–evasion games. In *Proceedings of the 2007 American Control Conference*, New York, NY, 2007, pp. 5316–5321.
2. Culler D, Estrin D and Srivastava M. Overview of sensor networks. *Computer* 2004; 37(8): 41–49.
3. Juang P, Oki H, Wang Y, Martonosi M, Peh L and Rubenstein D. Energy efficient computing for wildlife tracking: Design tradeoffs and early experiences with Zebranet. In *Proceedings of the 10th International Conference on Architectural Support for Programming Languages and Operating Systems (ASPLOS-X)*, 2002.
4. Hofner C and Schmidt G. Path planning and guidance techniques for an autonomous mobile cleaning robot. *Robotics Auton Syst* 1995; 14: 199–212.
5. Ferrari S, Fierro R, Perteet B, Cai C and Baumgartner K. A geometric optimization approach to detecting and intercepting dynamic targets using a mobile sensor network. *SIAM J Control Optimization* 2009; 48: 292–320.
6. Zhang G, Ferrari S and Qian M. Information roadmap method for robotic sensor path planning. *J Intell Robotic Syst* 2009; 56: 69–98.
7. Zhang G and Ferrari S. An adaptive artificial potential function approach for geometric sensing. In *Proceedings of the IEEE International Conference on Decision and Control*, 2009, pp.7903–7910.
8. Ferrari S and Cai C. Information-driven search strategies in the board game of clue. *IEEE Trans Syst Man Cybernet B* 2009; 39: 607–625.
9. Baumgartner K and Ferrari S. Optimal placement of a moving sensor network for track coverage. In *Proceedings of the American Control Conference*, New York, NY, 2007.
10. Isler V, Belta C, Daniilidis K and Pappas G. Hybrid control for visibility-based pursuit–evasion games. In *Proceedings of 2004 IEEE/RSJ International Conference on Intelligent Robots and Systems*, Sendai, Japan, 2004, pp.1432–1437.
11. Lulu L and Elnagar A. A comparative study between visibility-based roadmap path planning algorithms. In *IEEE/RSJ International Conference on Intelligent Robots and Systems, 2005 (IROS 2005)*, pp.3263–3268.
12. Bhattacharya S, Murrieta-Cid R and Hutchinson S. Optimal paths for landmark-based navigation by differential-drive vehicles with field-of-view constraints. *IEEE Trans Robotics* 2007; 23: 47–59.
13. Baumann M, Leonard S, Croft EA and Little JJ. Path planning for improved visibility using a probabilistic road map. *IEEE Trans Robotics* 2010; 26: 195–200.
14. Fierro R, Ferrari S and Tolic D. A geometric optimization approach to tracking maneuvering targets using a heterogeneous mobile sensor network. In *Proceedings of the IEEE Conference on Decision and Control*, Shanghai, P.R. China, 2009, pp.4004–4009.
15. BarsShalom Y, Li XR and Kirubarajan T. *Estimation with Applications to Tracking and Navigation: Algorithms and Software for Information Extraction*. New York: John Wiley and Sons, 2001.
16. BarsShalom Y and Blair WD. *Multitarget–Multisensor Tracking: Applications and Advances*. Norwood, MA: Artech House, 2000.
17. BarsShalom Y and Li XR. *Multitarget–Multisensor Tracking: Principles and Techniques*. YBS Publishing, 1995.
18. Blackman SS. *Multiple-Target Tracking with Radar Applications*. Norwood, MA: Artech House, 1986.
19. Morefield, C., ''Application of 0-1 integer programming to multitarget tracking problems,'' Automatic Control, IEEE Transactions on , vol.22, no.3, pp.302–312, Jun 1977.
20. Bishop G and Welch G. *An Introduction to the Kalman Filter*. Technical report, Department of Computer Science, University of North Carolina at Chapel Hill.
21. Julier SJ and Uhlmann JK. A new extension of the kalman filter to nonlinear systems. In *Proceedings AeroSense: 11th International Symposium Aerospace/Defense Sensing, Simulation and Controls*, 1997, pp.182–197.
22. Wan EA and Van Der Merwe R. The unscented Kalman filter for nonlinear estimation. In *Proceedings of the IEEE 2000 Adaptive Systems for Signal Processing, Communications, and Control Symposium*, 2000, pp.153–158.
23. Julier SJ. The scaled unscented transformation. In *Proceedings of the 2002 American Control Conference*, vol. 6, 2002, pp.4555–4559.
24. Khan Z, Balch T and Dellaert F. An mcmc-based particle filter for tracking multiple interacting targets. In Pajdla T and Matas J (eds), *Proceedings of Computer Vision - ECCV 2004*, 2004, pp.279–290.
25. Kreucher C, Kastella K and Hero O. Multitarget tracking using the joint multitarget probability density. *IEEE Trans Aerospace Electron Syst* 2005; 41: 1396–1414.
26. Arulampalam MS, Maskell S, Gordon N and Clapp T. A tutorial on particle filters for online nonlinear/non-Gaussian bayesian tracking. *IEEE Trans Signal Process* 2002; 50: 174–188.
27. Carpenter J, Clifford P and Fearnhead P. Improved particle filter for nonlinear problems. In *IEEE Proc Radar Sonar Navigation* 1999; 146: 2–7.
28. Yong Rui and Yunqiang Chen. Better proposal distributions: Object tracking using unscented particle filter. Computer Vision and Pattern Recognition, 2001. CVPR 2001. Proceedings of the 2001 IEEE Computer Society Conference on , vol.2, no., pp.II-786–II-793 vol.2, 2001.
29. Thomas W. O'Gorman. *Applied Adaptive Statistical Method: Test of Significance and Confidence Intervals*. Philadelphia, PA: Society for Industrial and Applied Mathematics, 2004.
30. Leung H, Hu Z and Blanchette M. Evaluation of multiple radar target trackers in stressful environments. *IEEE Trans Aerospace Electron Syst* 1999; 35: 663–674, 1999.
31. Cox IJ and Miller ML. On finding ranked assignments with application to multitarget tracking and motion correspondence. *IEEE Trans Aerospace Electron Syst* 1999; 31: 486–489.
32. Oprisan G and Limnios N. *Semi-Markov Process and Reliability*. Boston, MA: Birkhäuser, 2001.

33. Ren J and McIsaac K. A hybird-systems approach to potential field navigation for a multi-robot team. In *Proceedings IEEE International Conference on Robotics and Automation*, Taipei, Taiwan, 2003, pp.3875–3880.
34. Shimoda S, Kuroda Y and Iagnemma K. Potential field navigation of high speed unmanned ground vehicles on uneven terrain. In *Proceedings IEEE International Conference on Robotics and Automation*, 2005, pp.2839–2844.
35. Ge S and Cui Y. New potential functions for mobile robot path planning. *IEEE Trans Robotics Automat* 2000; 16(5): 615–620.
36. Latombe JC. *Robot Motion Planning*. Dordrecht: Kluwer Academic Publishers, 1991.
37. Yang Z, Zhang Q and Chen Z. Flocking of multi-agents with nonlinear inner-coupling function. *Nonlinear Dynamics* 2009; 60: 255–264.
38. Ge SS and Cui YJ. Dynamic motion planning for mobile robots using potential field method. *Auton Robots* 2002; 13: 207–222.
39. Khalil HK. *Nonlinear Systems*, 3rd edn. Englewood Cliffs, NJ: Prentice-Hall, 2000.
40. Mathworks. *Matlab*, 2004. http://www.mathworks.com.

Author Biographies

Wenjie Lu received a MS degree in mechanical engineering from Duke University, USA, in 2011, and BS degree in mechatronic engineering from Zhejiang University, China, 2009. His research focuses on intelligent mobile sensor agents that can adapt to heterogeneous environmental conditions, to achieve the optimal performance, such as demining and maneuvering target tracking. The mobile sensor agent is a robot with onboard sensors, and it is deployed to navigate obstacle-populated workspaces subject to sensing objectives. The expected performance of available future measurements is estimated using information theoretic metrics, and is optimized while minimizing the cost of operating the sensors, including distance. Approximate dynamic programming and particle filter techniques are studied to give the optimal control to the hybrid system.

Guoxian Zhang received a PhD degree in mechanical engineering from Duke University, USA, in 2011, and MS degree in mechanical engineering from Tsinghua University, Beijing, China, 2006. His research focuses on intelligent mobile sensors that can adapt to heterogeneous environmental conditions, to achieve the optimal performance. Robots with onboard sensors navigate obstacle-populated workspaces for the purpose of measuring hidden targets, and infer their classification. The expected performance of available future measurements is estimated using information theoretic metrics, and is optimized while minimizing the cost of operating the sensors, including distance. When sensors of limited range navigate a workspace with potential targets, both the sensors and the targets can be represented by probability density functions, and their performance measured by their track coverage. Sensor networks can thus be considered as information gathering systems, that make decisions based on the environment and prior information, and can learn to optimize their performance over time using techniques from data mining and machine learning.

Silvia Ferrari is Paul Ruffin Scarborough Associate Professor of Engineering at Duke University, where she directs the Laboratory for Intelligent Systems and Controls (LISC). Her principal research interests include robust adaptive control of aircraft, learning and approximate dynamic programming, and optimal control of mobile sensor networks. She received the BS degree from Embry-Riddle Aeronautical University and the MA and PhD degrees from Princeton University. She is a senior member of the IEEE, and a member of ASME, SPIE, and AIAA. She is the recipient of the ONR young investigator award (2004), the NSF CAREER award (2005), and the Presidential Early Career Award for Scientists and Engineers (PECASE) award (2006).

Mike Anderson is pursuing his Masters Degree in Electrical Engineering at the University of New Mexico, where he works on research projects in the Multi-Agent, Robotics, Hybrid, and Embedded Systems (MARHES) Laboratory at UNM. He is also employed by Sandia Staffing Alliance working under contract to Sandia National Laboratories. His research interests include multi-agent systems utilizing both ground and aerial agents to perform sensing and target tracking tasks cooperatively, hybrid dynamic systems, optimal and robust control, adaptive dynamic programming, and machine learning. He received a BS degree in Electrical Engineering from the University of New Mexico.

Rafael Fierro is an Associate Professor of the Department of Electrical and Computer Engineering, University of New Mexico where he has been since 2007. He received a MSc degree in control engineering from the University of Bradford, England and a PhD degree in electrical engineering from the University of Texas–Arlington. Prior to joining UNM, he held a postdoctoral appointment with the GRASP Lab at the University of Pennsylvania and a faculty position with the Department of Electrical and Computer Engineering at Oklahoma State University. His research interests include cooperative control of multi-agent systems, mobile sensor and robotic networks, motion planning under sensing/communication constraints, multivehicle coordination, cyber-physical systems, and dynamic information flow tracking in computer security. He directs the Multi-Agent, Robotics, Hybrid and Embedded Systems (MARHES) Laboratory. He was the recipient of a Fulbright Scholarship, a 2004 National Science Foundation CAREER Award, and the 2007 ISA Transactions Best Paper Award. He is serving as Associate Editor for the *IEEE Control Systems Magazine* and *IEEE Transactions on Automation Science and Engineering*.